Available online at www.sciencedirect.com
SCIENCE DIRECT®

Radiation Measurements 41 (2006) 101–107

Radiation Measurements

www.elsevier.com/locate/radmeas

Exposures to ^{222}Rn and its progeny derived from implanted ^{210}Po activity

D. Nikezić[1], K.N. Yu*

Department of Physics and Materials Science, City University of Hong Kong, Tat Chee Avenue, Kowloon Tong, Kowloon, Hong Kong

Received 7 October 2004; received in revised form 22 January 2005; accepted 7 March 2005

Abstract

The Jacobi room model was applied to study the relative contributions from the unattached and attached fractions to the implanted activity of ^{210}Po. It was found that under normal conditions, about 85% of the implantation was due to the unattached fraction. Sensitivity analysis was performed to identify the most important factors that influence the deposition and implantation of radon progeny. The main factors affecting the incorporation of ^{210}Po are the attachment rate, deposition rate of unattached progeny and the surface to volume ratio of the room. The calibration curves, which related the ^{210}Po activity per unit surface area to the concentrations of ^{222}Rn and of the radon progeny, were determined as functions of exposure times. The implanted activity is found to distribute close to a lognormal distribution. For an exposure of 20 years, the distribution has a geometric standard deviation of 2.2 and a geometric mean of $0.023\,\mathrm{Bq/m^2/(Bq/m^3)}$. The last value is considered as the calibration coefficient of the glass response in terms of the implanted ^{210}Po activity per unit surface area per unit concentration of ^{222}Rn for an exposure period of 20 years.

Keywords: Radon; Radon progeny; ^{210}Po; Implantation; Retrospective dosimetry

1. Introduction

Methods for long-term passive radon measurements based on nuclear track detectors have been very well established and widely used. A survey of existing techniques has been given by Nikolaev and Ilić (1999) and Nikezić and Yu (2004). Although these are classified as long-term measurement methods, the duration of measurements usually range between a few months to one year and are still too short compared to the average lifespan of a person. For risk estimation for a person (e.g., Bochicchio et al., 2003; Nikezić and Yu, 2005), the total cumulative exposure is needed, so measurements performed for a few months might not be representative. As a possible solution to this problem, retrospective dosimetry based on measurements of ^{210}Po activity in objects was proposed. Atoms of short-lived ^{222}Rn progeny, namely, ^{218}Po, ^{214}Pb, ^{214}Bi and ^{214}Po, can deposit on internal surfaces of a room. Due to the recoil after α decays of the ^{218}Po and ^{214}Po nuclides, some of the newly formed atoms (^{214}Pb and ^{210}Pb) can be incorporated into the surface. The activity of the long-lived ^{210}Pb ($T_{1/2} = 22.3\ y$) accumulated in a surface increases with the time of exposure. The activity of the second successor of ^{210}Pb, which is ^{210}Po and is α-particle emitting, can be determined through α measurements.

Methods were developed for determining the retrospective ^{222}Rn exposure based on measurements of the ^{210}Po activity in an object by using various techniques of α-activity

* Corresponding author: Tel.: +852 27887812; fax: +852 27887830.
E-mail address: peter.yu@cityu.edu.hk (K.N. Yu).
[1] On leave from Faculty of Science, University of Kragujevac, Serbia and Monte Negro.

1350-4487/$ - see front matter © 2005 Elsevier Ltd. All rights reserved.
doi:10.1016/j.radmeas.2005.03.004

measurements (Lively and Ney, 1987; Samuelsson, 1988; Mahaffey et al., 1993; Samuelsson and Johansson, 1994; McLaughlin, 1998). It was established that the α-activity of ^{210}Po is related to the cumulative ^{222}Rn exposure. Various glass objects were found to be useful for this purpose. The influence of dust on the implantation of recoil ^{222}Rn progeny atoms was studied by Johansson et al. (1994). Roos and Whitlow (2003) analyzed the depth distribution of the implanted activity in order to obtain information about factors that affect the implantation of radon progeny into glass. By comparing the experimental and calculated distributions, they showed that diffusion of implanted atoms and cleaning did not significantly affect the total activity of ^{210}Po or its depth distribution. A review of the retrospective radon dosimetry has been given by Nikezić and Yu (2004).

The objective of this paper is to investigate the influence of different room parameters on the amount of implanted radon progeny in an object such as a glass object. The average calibration coefficient, which relates the implanted ^{210}Po activity to the exposure to radon or to radon progeny, will be determined from calculations.

Sensitivity analysis of the implanted ^{210}Po activity on different parameters will also be carried out in this paper. A similar analysis was performed earlier by Walsh and McLaughlin (2001) but with somewhat different methodologies and different ranges of used parameters. A comparison between our results with their results will be given in the discussions.

2. Contributions to the implanted activity from the unattached and attached fractions

Nikezić and Yu (1999, 2000) derived the formula for the total deposition flux, $r_{\rm tot}$, defined as the total number of radon progeny atoms deposited onto a unit surface area in a unit time (given in *number of deposited atoms*/(m^2 *s*)) as

$$r_{\rm tot} = r_1 + r_2 + r_3 = \frac{V}{S}\left[\lambda_{\rm d}^{\rm u}\left(\frac{A_1^{\rm u}}{\lambda_1} + \frac{A_2^{\rm u}}{\lambda_2} + \frac{A_3^{\rm u}}{\lambda_3}\right) + \lambda_{\rm d}^{\rm a}\left(\frac{A_1^{\rm a}}{\lambda_1} + \frac{A_2^{\rm a}}{\lambda_2} + \frac{A_3^{\rm a}}{\lambda_3}\right)\right], \tag{1}$$

where r_i is deposition flux for the ith progeny ($i = 1, 2, 3$ for ^{218}Po,^{214}Pb and ^{214}Bi, respectively), $\lambda_{\rm d}^{\rm u}$ and $\lambda_{\rm d}^{\rm a}$ are deposition rates of the unattached and attached progeny, *V/S* is the volume to surface ratio of a room, λ_i are decay constants and A_i are activity concentrations of progeny in Bq/m^3. The first term in the square brackets represents the contribution from the unattached fraction and the second term represents the contribution from the attached fraction. To estimate the relative contributions from the unattached and attached fractions, a small computer program based on the Jacobi room model (Jacobi, 1972) was written and run. The following equations for the Jacobi model were used:

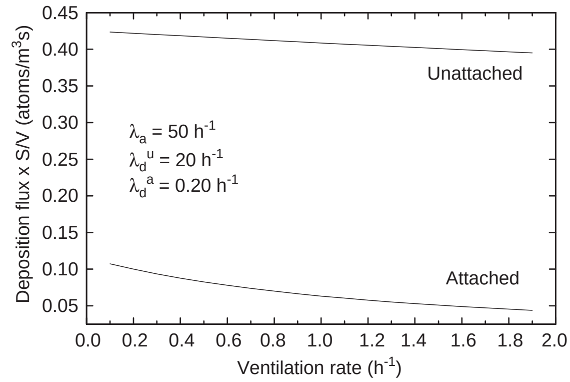

Fig. 1. Variation of the deposition flux of the unattached and attached progeny with the ventilation rate.

$$f_i^{\rm u} = \frac{\lambda_i (f_{i-1}^{\rm u} + p_{i-1} f_{i-1}^{\rm a})}{\lambda_i + \lambda_{\rm v} + \lambda_{\rm a} + \lambda_{\rm d}^{\rm u}}, \tag{2}$$

$$f_i^{\rm a} = \frac{\lambda_{\rm a} f_i^{\rm u} + (1 - p_{i-1})\lambda_i f_{i-1}^{\rm a}}{\lambda_i + \lambda_{\rm v} + \lambda_{\rm d}^{\rm a}}, \tag{3}$$

where $f_i^{\rm u}$ and $f_i^{\rm a}$ are the ratios of the activity concentrations of the unattached progeny and attached progeny, respectively, to that of radon, $\lambda_{\rm v}$ is the ventilation rate and $\lambda_{\rm a}$ is the attachment rate (Amgarou et al., 2003). The recoil factor p_{i-1} was taken as 0.83 after α decay and 0 after β decay.

Although the parameters mentioned above have typical values, they have rather wide ranges. To estimate the relative contributions from the unattached and attached fractions, the following approach was used. All parameters were kept at their typical values except one that was varied within its own range. The radon concentration was taken to be 1 Bq/m^3. Through Eqs. (2) and (3), the ratios $f_i^{\rm u}$ and $f_i^{\rm a}$ were calculated and the contributions from the unattached fraction,

$$\lambda_{\rm d}^{\rm u}\left(\frac{A_1^{\rm u}}{\lambda_1} + \frac{A_2^{\rm u}}{\lambda_2} + \frac{A_3^{\rm u}}{\lambda_3}\right)$$

and from the attached fraction,

$$\lambda_{\rm d}^{\rm a}\left(\frac{A_1^{\rm a}}{\lambda_1} + \frac{A_2^{\rm a}}{\lambda_2} + \frac{A_3^{\rm a}}{\lambda_3}\right),$$

were then determined.

In Fig. 1, the results are given for variable ventilation rates. The ventilation rate was varied from 0.1 to 2 h^{-1}, while the other parameters were kept at their typical values as shown in Fig. 1. One can see that the contribution from the unattached fraction is significantly larger than that from the attached fraction. If all parameters are kept at their best estimates, deposition of the unattached fraction was dominant over a wide range of ventilation rates.

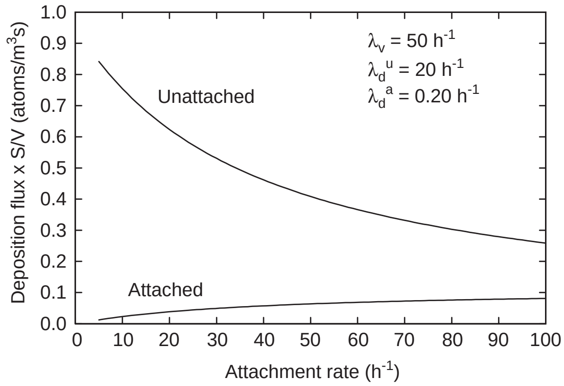

Fig. 2. Variation of the deposition flux of the unattached and attached progeny with the attachment rate.

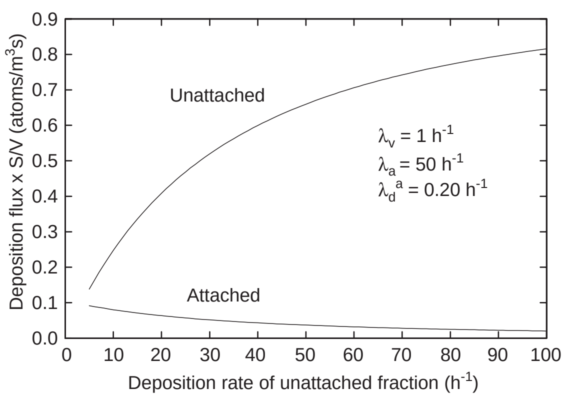

Fig. 3. Variation of the deposition flux of the unattached and attached progeny with the deposition rate of the unattached progeny.

In Fig. 2, the dependence of the deposition flux on the attachment rate is given. Again the contribution is larger from the unattached progeny than from the attached progeny. With increasing attachment rate, the contributions get closer to each other. At larger attachment rates, the unattached fraction decreases and the attached fraction increases, and contributions to the deposition flux follow this trend. Larger attachment rates are expected for "dusty" atmospheres with larger aerosol concentrations.

In Fig. 3, the dependence of the deposition flux on the deposition rate of unattached progeny is given. Again, the contribution from the unattached fraction is much larger than that for attached fraction, except for very small values of λ_d^u. With the increase in the deposition rate of the attached progeny (see Fig. 4), the difference between the contributions from the unattached and attached fractions becomes smaller. However, it is not very reasonable to assume that only one deposition rate will increase, while the other will be constant as is the case for Fig. 4. Deposition velocities depend on the characteristics of air movement inside the room. In this way, if one deposition velocity increases, the other would probably increase as well.

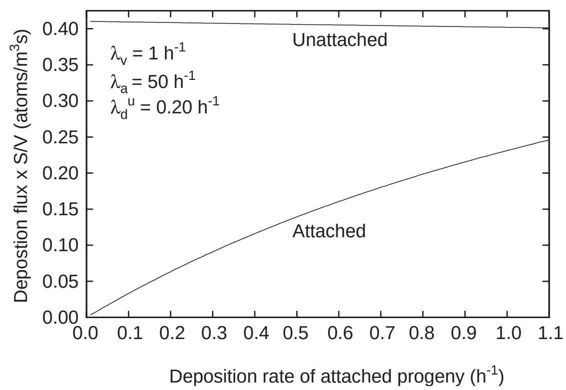

Fig. 4. Variation of the deposition flux of the unattached and attached progeny with the deposition rate of the unattached progeny.

From the previous results, it is noted that the contribution from the unattached fraction to the total deposition flux is much larger than that from the attached fraction, except only in some extreme cases. As a conclusion of this section, the activity of ^{210}Po implanted in objects, e.g., glass, is mainly due to deposition of the unattached fraction. If all parameters are kept at their best estimates ($\lambda_v = 0.55\,\mathrm{h}^{-1}$, $\lambda_a = 50\,\mathrm{h}^{-1}$, $\lambda_d^u = 20\,\mathrm{h}^{-1}$ and $\lambda_d^a = 0.2\,\mathrm{h}^{-1}$), the contributions are about 85% from the unattached progeny and about 15% from the attached progeny.

3. Total activity of ^{210}Po

3.1. Activity ratio between ^{210}Po/^{210}Pb

The total activity, A_5, of ^{210}Pb implanted in an object is given as

$$A_5 = \frac{r_1 + r_2 + r_3}{2}(1 - e^{-\lambda_5 t}), \tag{4}$$

where λ_5 is the half-life of ^{210}Pb (Nikezić and Yu, 1999, 2000). The index 5 is used because ^{210}Pb is the fifth member of the decay chain after ^{222}Rn. If equilibrium is established, the activity A_7 of the seventh-radon progeny, ^{210}Po, is equal to A_5. For shorter exposure time, equilibrium is not established and the full system of differential equations that describes the growth of implanted progeny in glass has to be solved. The variation of the number, N_6, of atoms per unit surface area of the sixth-radon progeny, ^{210}Bi, with time is given by the equation

$$\frac{dN_6}{dt} = \lambda_5 N_5 - \lambda_6 N_6 \tag{5}$$

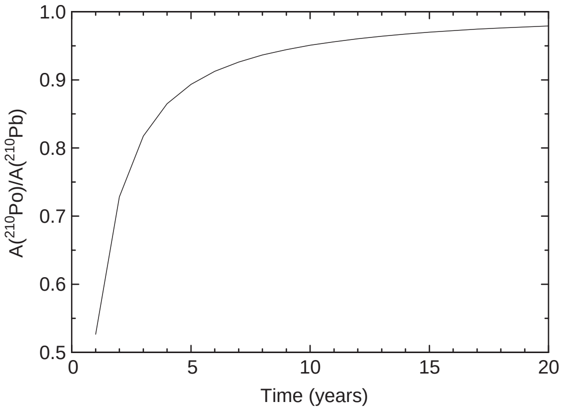

Fig. 5. Activity ratio between ^{210}Po/ ^{210}Pb as a function of exposure time in an object.

with the solution of

$$N_6 = \frac{r_{tot}}{2}\left[\frac{e^{-\lambda_6 t} - e^{-\lambda_5 t}}{\lambda_6 - \lambda_5} + \frac{1 - e^{-\lambda_6 t}}{\lambda_6}\right]. \quad (6)$$

Variation of the number of atoms, N_7, of ^{210}Po with time is given by the differential equation

$$\frac{dN_7}{dt} = \lambda_6 N_6 - \lambda_7 N_7 \quad (7)$$

with a rather complicated solution as

$$A_7 = \frac{r_{tot}\lambda_7}{2}\left[\frac{\lambda_6(e^{-\lambda_6 t} - e^{-\lambda_7 t})}{(\lambda_6 - \lambda_5)(\lambda_7 - \lambda_6)} + \frac{\lambda_6(e^{-\lambda_7 t} - e^{-\lambda_5 t})}{(\lambda_6 - \lambda_5)(\lambda_7 - \lambda_5)} + \frac{(e^{-\lambda_7 t} - e^{-\lambda_6 t})}{(\lambda_7 - \lambda_6)} + \frac{1}{\lambda_7}(1 - e^{-\lambda_7 t})\right]. \quad (8)$$

Eqs. (4) and (8) were used to calculate the activities of ^{210}Po and ^{210}Pb implanted in glass. The variation of the activity ratio between ^{210}Po and ^{210}Pb with time is shown in Fig. 5. From Fig. 5, we observe that about 6 years of exposure is needed to establish a 90% equilibrium between ^{210}Po and ^{210}Pb implanted in the glass object.

3.2. Sensitivity of implanted ^{210}Po activity to different room parameters

To identify the most important factor affecting the accumulation of ^{210}Pb and ^{210}Po, the following approach was used. The radon concentration was taken as a constant and equal to $1\,\mathrm{Bq/m^3}$, while other parameters of the Jacobi model were changed within their typical ranges and A_7 was calculated for a unit radon concentration for an exposure period of 20 years.

The sensitivity factor, s, is defined as the square root of the ratio between the largest value (A_7^{max}) and the smallest value (A_7^{min}) of A_7, i.e.,

$$s = \sqrt{\frac{A_7^{max}}{A_7^{min}}}. \quad (9)$$

The s values for various Jacobi room model parameters are given in Table 1, which are obtained for the activity of ^{210}Po implanted on a unit surface area of an object per $1\,\mathrm{Bq/m^3}$ of ^{222}Rn, i.e., (Bq of ^{210}Po/m^2)/(Bq of ^{222}Rn/m^3), for an exposure of 20 years. Three values of A_7 are given in Table 1 for each parameter, namely, for the minimum, typical and maximum values of the parameter. The sensitivity factors are given in the last column of Table 1. The ranges of parameters and their typical values used in Table 1 followed those used by Amgarou et al. (2003).

Surprisingly, the largest s of 2.04 was obtained for the attachment rate. This may be a consequence of the very wide range for this parameter. A somewhat smaller s (1.81) was obtained for the deposition rate for the unattached fraction. The incorporated activity was less influenced by the deposition rate of the attached progeny, where s was 1.26. The smallest s occurs for the ventilation rate. This can be explained as follows. The present results were given for a unit ^{222}Rn activity. While the radon gas activity is strongly influenced by ventilation, the ratio of radon progeny to radon concentration is not. Therefore, the deposition flux and consequently A_7 for a constant radon concentration is not influenced significantly by ventilation. The ^{210}Po activity is directly proportional to *V/S*, i.e., the volume to surface ratio of a room. By increasing *V/S* (or equivalently decreasing *S/V* which is shown in Table 1), a relatively smaller surface area is available for deposition, which will increase the deposition and incorporated activity per unit surface area.

3.3. Distribution of implanted activity and calibration curve for ^{222}Rn exposure

In this section, we would like to study the case when all the parameters for the Jacobi room model were changed simultaneously and randomly between the minimum and maximum values given in Table 1. Uniform distributions of the parameters were assumed because there was no better information available. For each combination of parameters, the implanted activity of ^{210}Po was calculated assuming that the ^{222}Rn concentration is $1\,\mathrm{Bq/m^3}$ and that exposure lasts 20 years. The implanted activities were sorted into 100 intervals to give a frequency distribution, the frequencies of which were further divided with the total number of cases (which was 4×10^6 in our calculations) to give the probability distribution. The probability values in the probability distribution were then divided by the width of the intervals to give the distribution density as shown in Fig. 6.

Although the parameters had wide ranges of values, the obtained distribution of implanted ^{210}Po was relatively sharp. The maximal value is about $0.1\,\mathrm{Bq/m^2}$ of ^{210}Po for an irradiation of 20 years to $1\,\mathrm{Bq/m^3}$ of ^{222}Rn

Table 1
Variations of the implanted ^{210}Po activities (A_7) as the Jacobi room model parameters change among the minimum, typical and maximum values, and the obtained sensitivity factors

Parameter/activity	Minimum value	Typical value	Maximum value	$\sqrt{\frac{A_7^{max}}{A_7^{min}}}$
$\lambda_a (h^{-1})$	5	50	500	
$A_7 (Bq/m^2)/(Bq/m^3)$	0.05	0.028	0.012	2.04
$\lambda_d^u (h^{-1})$	5	20	110	
$A_7 (Bq/m^2)/(Bq/m^3)$	0.015	0.028	0.049	1.81
$S/V (m^{-1})$	2	4	6	
$A_7 (Bq/m^2)/(Bq/m^3)$	0.056	0. 028	0.019	1.72
$\lambda_d^a (h^{-1})$	0.05	0.2	1.1	
$A_7 (Bq/m^2)/(Bq/m^3)$	0.025	0.028	0.040	1.26
$\lambda_v (h^{-1})$	0.1	0.55	2	
$A_7 (Bq/m^2)/(Bq/m^3)$	0.030	0.028	0.025	1.10

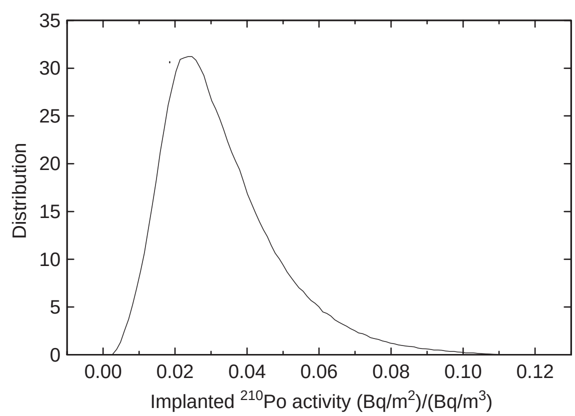

Fig. 6. Distribution of the implanted ^{210}Po activity when all the parameters in the Jacobi room model are changed simultaneously and randomly between the minimum and maximum values, assuming uniform distributions of the parameters.

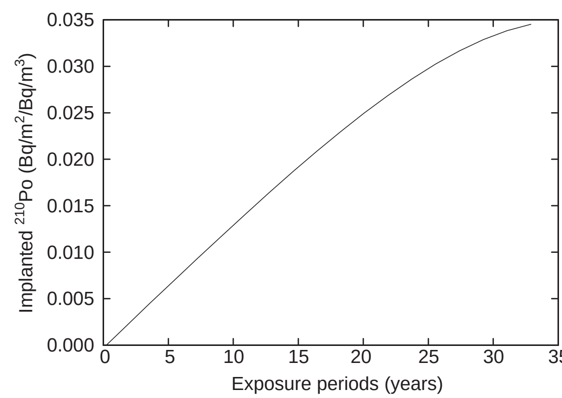

Fig. 7. Calibration curve showing the relationship between the activity of implanted ^{210}Po (in Bq/m^2) per unit activity of ^{222}Rn (Bq/m^3) as a function of the exposure period.

(largest x value). The distribution has a maximum at $A_7 = 0.023\,Bq/m^2$ of ^{210}Po but the average value is shifted to $0.032\,Bq/m^2$ because the distribution has a tail on the right side. The curve shown in Fig. 6 is very close to a lognormal distribution. Fitting the data in Fig. 6 according to a lognormal distribution gave a geometric standard deviation σ_g of 2.02 and a geometric mean of 0.023 (Bq/m^2 of ^{210}Po)/(Bq/m^3 of ^{222}Rn). The range from 0.011 to 0.046 Bq/m^2, obtained from (0.023/2.02) and (0.023 × 2.02) Bq/m^2, then covers about 68% of the cases.

The value of 0.023 (Bq/m^2 of ^{210}Po)/(Bq/m^3 of ^{222}Rn) can be considered as a calibration coefficient. However, this result is valid only for an exposure of 20 years. In practice, it is difficult to find an object that is exposed for exactly 20 years. In order to determine the calibration coefficient for other exposure periods, the previous procedures were repeated with steps of 1 year and the results are given as a calibration curve in Fig. 7. The calibration coefficient for the exposure of 1 year, obtained by simultaneous varying of all parameters was 0.00086 $(Bq/m^2)/(Bq/m^3)$.

If *typical* values were adopted for all parameters of the model and exposure time was 1 year, the implanted ^{210}Po activity calculated by our program was 0.00086 $(Bq/m^2)/(Bq/m^3)$. Walsh and McLaughlin (2001) obtained about $0.45\,Bq/m^2$ of ^{210}Po for an exposure of $500\,Bq/m^3$ for 1 year, which would lead to a corresponding

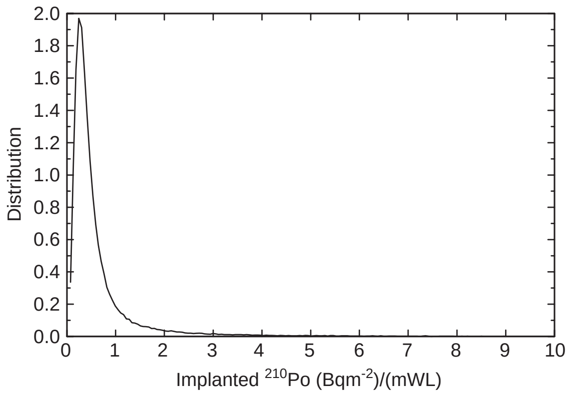

Fig. 8. Distribution of implanted ^{210}Po activity per unit radon progeny concentration (PAEC in mWL) for an exposure of 20 years.

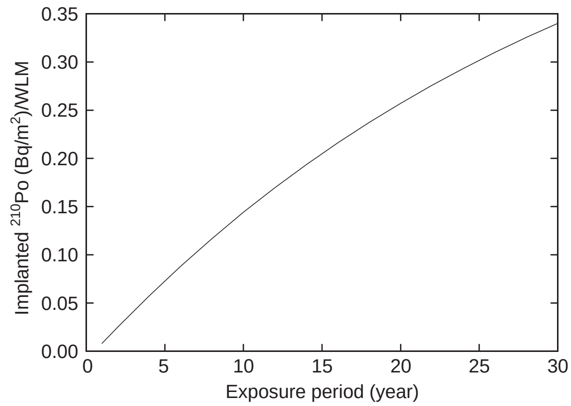

Fig. 9. Calibration curve showing the relationship between the activity of implanted ^{210}Po (in Bq/m^2) per unit potential α energy concentration (PAEC in WL) as a function of the exposure period.

value of 0.0009 (Bq/m^2)/(Bq/m^3). Although the adopted distributions have been different (i.e., a lognormal distribution used by Walsh and McLaughlin (2001) and a uniform distribution in the present work), and the considered ranges of the parameters have not been the same, the obtained results are close to each other.

3.4. Calibration curve for progeny exposure

The procedures related to radon exposure described in the previous section were repeated for radon progeny concentrations, which were expressed through the potential α energy concentration (PAEC), which is the sum of the attached and the unattached fractions. The PAEC is usually expressed with the traditional unit working level (WL). The results obtained for an exposure of 20 years are given in Fig. 8.

The distribution in Fig. 8 is much more skewed than previous one. A very sharp peak occurs at 0.3 Bq/m^2/m WL. The distribution falls quickly as the implanted activity is close to zero, but there is a long tail towards larger values of implanted activities. Fitting the data in Fig. 8 according to the lognormal distribution gave a geometric standard deviation $\sigma_g = 2.2$ and a geometric mean of 0.26 Bq/m^2/m WL. The average value was 0.67 Bq/m^2/m WL.

The procedures were then repeated for different exposure periods and the geometric mean values are presented in Fig. 9 as a function of time. It is noted that both the calibration curves for radon and for radon progeny are close to linear. However, both curves show a slower increasing rate at longer exposure time, which is due to the decay of ^{210}Pb.

4. Discussion and conclusions

Sensitivity analyses were performed earlier by Walsh and McLaughlin (2001). Walsh and McLaughlin (2001) used two methods to analyze the importance of the various parameters in the Jacobi room model. In the first approach, one parameter was varied within a realistic range of values, and all other parameters were kept at their typical values. In the second approach, they applied the Monte Carlo method to determine the distribution of the model output by simultaneously changing all parameters. The output from their calculations was the *radon concentration* obtained from the ^{210}Po activity on an object, and the variability factor was defined in terms of the radon concentration. In summary, their results answered the question how different parameters affect the estimated radon concentration from the known ^{210}Po activity on an object.

In our approach described in the present paper, we assumed a constant radon concentration and the output was the implanted ^{210}Po activity, A_7, and the sensitivity factor was expressed through A_7. In summary, the present work attempted to answer the question how different parameters affect the implanted activity of ^{210}Po. In essence, the present approach is opposite to that of Walsh and McLaughlin (2004). Nevertheless, both approaches enable determination of the calibration coefficient.

In addition, there are differences in the parameters used in the two analyses. Walsh and McLaughlin (2001) varied the aerosol concentration and deposition velocities of unattached and attached progeny while we varied the attachment rate and the deposition rate instead. Furthermore, we identified the deposition rate of unattached progeny as the most critical parameter while Walsh and McLaughlin (2001) found the unattached deposition velocity as the most important one. These two findings are in fact commensurate with each other because the deposited fraction is proportional to the deposition velocity. The ranges of other parameters used in the two works (given here in Table 1) are similar but not exactly the same.

Both works, Walsh and McLaughlin (2001) and the present one, found that the parameter with the smallest influence on the method was the ventilation rate. Slightly different ranges and typical values for the ventilation rate were used, viz., Walsh and McLaughlin (2001) used 0.2–1.5 h^{-1} with a typical value of 0.5, and we used 0.1–2 h^{-1} with a typical 0.55 h^{-1}.

The Monte Carlo approach was employed in both works. Walsh and McLaughlin (2001) used lognormal distributions for the aerosol concentration, ventilation rate, deposition rates and AMADs, and a uniform distribution for surface to volume ratio. In the present work, we used uniform distributions for the deposition rate, attachment rate, the ventilation rate and the volume to surface ratio. One output from the calculations, namely, the calibration coefficient for an exposure of 1 year, could be compared and was found to be similar in both works. It seems that the choice of distribution for individual parameters is not very critical for the average value of implanted ^{210}Po activity, but the situation could be quite different for the distribution width.

The relationship between the implanted ^{210}Po activity and PAEC is given by Walsh and McLaughlin (2001) as a scatter plot and direct comparison with our results is not possible. From their scatter plot, about 10 Bq/m^2 of ^{210}Po is estimated for a PAEC of 30 Bq/m^3, which is approximately equivalent to 0.8 Bq/m^2 per mWL (if equilibrium factor = 1). This value is about three times larger than the geometric mean of our distribution (0.26 Bq/m^2/m WL) but it is comparable to the average value of our distribution (0.67 Bq/m^2/m WL).

In the present work, the Jacobi room model was applied to study the relative contributions from the unattached and attached fractions to the implanted activity of ^{210}Po. It was found that under normal conditions, 85% of the implantation was due to the unattached fraction. The incorporated ^{210}Po activities in glass objects form an estimator of the unattached fraction. However, determination of partitioning between the contribution from the unattached and the attached fraction is not possible based on activity measurements alone. The main factors affecting the incorporation of ^{210}Po are the attachment rate, deposition rate of unattached progeny and the volume to surface area ratio of the room.

The calibration curve, which related the ^{210}Po activity per unit surface area to the ^{222}Rn concentration, was determined for various exposure periods. The glass response in terms of the implanted ^{210}Po activity per unit surface area per unit concentration of ^{222}Rn was 0.023 $Bq/m^2/(Bq/m^3)$ for an exposure period of 20 years. It is, however, remarked that the parameters in the Jacobi room model might have distributions different from the rectangular distribution, and that some parameters are not independent with one another. Such assumptions were made because no better information could be obtained at the present time. Another calibration curve, which related the surface ^{210}Po activity to the average radon progeny concentrations, was also derived. Both the calibration curves, relating the surface ^{210}Po activity to the radon and radon progeny concentrations, were close to linear. However, both curves showed a slower increasing rate at longer exposure time due to the decay of ^{210}Pb.

Acknowledgements

This research was supported by a grant from the Research Grants Council of the Hong Kong Special Administrative Region, China [Project no. CityU 103204].

References

Amgarou, K., Font, Ll., Baixeras, C., 2003. A novel approach for long-term determination of indoor ^{222}Rn progeny equilibrium factor using nuclear track detectors. Nucl. Instrum. Methods A 506, 186–198.

Bochicchio, F., Forastiere, F., Farchi, S., Marocco, D., Quarto, M., Sera, F., 2003. Quality assurance program for LR 115 based radon concentration measurements in a case-control study: description and results. Radiat. Meas. 36, 205–210.

Jacobi, W., 1972. Activity and potential α energy of ^{222}Rn and ^{220}Rn daughters in different air atmosphere. Health Phys. 22, 441–450.

Johansson, L., Wolff, M., Samuelsson, C., 1994. The influence of dust on the ^{210}Po signal in retrospective Rn dosimetry. Radiat. Prot. Dosim. 56, 141–143.

Lively, R.S., Ney, E.P., 1987. Surface radioactivity resulting from the deposition of ^{222}Rn daughter products. Health Phys. 52, 411–415.

Mahaffey, J.A., Parkhurst, M.A., James, A.C., Cross, F.T., Alavanja, M.C.R., Boice, J.D., Ezrine, S., Henderson, P., Brownson, R.C., 1993. Estimating past exposure to indoor Rn from household glass. Health Phys. 64, 381–391.

McLaughlin, J.P., 1998. The application of techniques to assess radon exposure retrospectively. Radiat. Prot. Dosim. 78, 1–6.

Nikezić, D., Yu, K.N., 1999. Modelling radon progeny behaviour on surfaces and note on radon retrospective dosimetry. Radiat. Prot. Dosim. 82, 141–146.

Nikezić, D., Yu, K.N., 2000. Relationship between the ^{210}Po activity incorporated in the surface of an object and the potential α-energy concentration. J. Environ. Radioact. 47, 45–55.

Nikezić, D., Yu, K.N., 2004. Formation and growth of tracks in nuclear track materials. Mater. Sci. Eng. R. 46, 51–123.

Nikezić, D., Yu, K.N., 2005. Are radon gas measurements adequate for epidemiological studies and case control studies of radon induced lung cancer? Radiat. Prot. Dosim. 113, 233–235.

Nikolaev, V.A., Ilić, R., 1999. Etched track radiometers in radon measurements: a review Radiat. Meas. 30, 1–13.

Roos, B., Whitlow, H.J., 2003. Computer simulation and experimental studies of implanted ^{210}Po in glass resulting from radon exposure. Health Phys. 84, 72–81.

Samuelsson, C., 1988. Retrospective determination of Rn in houses. Nature 334, 338–340.

Samuelsson, C., Johansson, L., 1994. Long lived Rn decay products as a long term Rn exposure indicator. Radiat. Prot. Dosim. 56, 123–126.

Walsh, C., McLaughlin, J.P., 2001. Correlation of ^{210}Po implanted in glass with radon gas exposure: sensitivity analysis of critical parameters using Monte Carlo approach. Sci. Total Environ. 272, 195–202.